RC23726 (W0509-095) September 27, 2005
Other

IBM Research Report

Aspects of the Controlled Chemical Etching of Thin Metal Films, in Particular Multilayer Type

E. J. O'Sullivan
IBM Research Division
Thomas J. Watson Research Center
P.O. Box 218
Yorktown Heights, NY 10598

Research Division
Almaden - Austin - Beijing - Haifa - India - T. J. Watson - Tokyo - Zurich

ASPECTS OF THE CONTROLLED CHEMICAL ETCHING OF THIN METAL FILMS, IN PARTICULAR MULTILAYER TYPE

E. J. O'Sullivan

IBM/Infineon MRAM Development Alliance
IBM Research Division
Thomas J. Watson Research Center
P.O. Box 218
Yorktown Hts., NY 10598, USA

ABSTRACT

This paper first discusses an application of chemical etching for selective patterning of magnetic soft (or free) layers, principally Permalloy, in MRAM stacks. Passive films formed in the prior cap layer patterning step played a critical role in the etching behavior of the magnetic layers. The novel use of a sulfur-based additive to inhibit Permalloy passivation, thus enabling selective etching in weak acid etchants, was demonstrated. Aqueous etch solutions of α, ω-dicarboxylic acids were found to etch Permalloy films whose surfaces contained a chemisorbed, sulfur-based, passivation inhibitor, but left the alumina tunnel barrier intact. High values of array quality factors for magnetic switching were demonstrated for chemically etched arrays of Permalloy elements. In the second part of the paper, a discussion of self-assembled monolayers as masks for chemical etching is presented, and the paper concludes with a brief review of the role of passive films in chemical mechanical planarization.

INTRODUCTION

Wet chemical processing, which includes dielectric and metal etching, and post-reactive ion etch (RIE) cleaning, plays a vital role in the microelectronics industry. A modern Fab contains a multitude of front and back-end-of-line (FEOL and BEOL) wet processing tools. BEOL wet processing has become increasingly important as the number of metal levels has increased, and feature sizes have relentlessly shrunk. The presence of a metal layer often precludes the use of some of the aggressive chemical solutions (e.g., HF-based) used in the FEOL. Furthermore, in the coming years, backend processing is expected to include increasing involvement of non-traditional products, for example, nonvolatile memory type, such as tunnel junction-based magnetic random access memory (MRAM). The latter's stack currently contains two – four, thin ferromagnetic layers.

This paper will first focus on the controlled chemical etching of thin MRAM-type films of metals and alloys, e.g., ferromagnetic type, with emphasis on inhibition by passive films, etch selectivity, and avoidance of Galvanic effects. Following a discussion

of self-assembled monolayers as masks for chemical etching, the paper will conclude with a brief review of the role of passive films in chemical mechanical planarization.

The chemical etching of metals involves both localized anodic (metal oxidation) and cathodic (oxidant reduction) reactions. Corrosion is an unwanted form of metal etching or reaction. The cathodic reaction is a critical, enabling feature of metal etching (and of corrosion). It is influenced by several factors, including the following: the standard potential of the oxidant; the concentration of the oxidant in solution; rate-limiting mass transfer, which influences etching rate uniformity; in the case of Galvanic effects, the difference in, a) the area, and b) the kinetics of oxidant reduction, of the surface supporting the cathodic reactions relative to the surface undergoing etching; and, the presence of inhibition films.

This first part of this paper contains an detailed review of the selective etching of MRAM magnetic tunnel junction (MTJ) free layer etching with an emphasis on the importance of passive films in the etching process. The second part review aspects of the chemical etching of metal films in other systems, with an emphasis on the role of inhibiting films on the etching process.

MTJ-BASED SOFT LAYERS

Magnetic tunnel junctions (MTJ) show much promise for magnetic random access memory (MRAM) (1,2). This is principally due to nonvolatility (memory retention without power consumption), high read and write cycles of a few nanoseconds duration, and eventually high memory density (bits per unit area) approaching that of dynamic random access memory (DRAM).

Magnetic tunnel junctions (1, 2), which are of submicron dimensions, possess thin ferromagnetic films. Their 20-50 Å z-direction thickness relative to the x-y dimensions of patterned MTJ elements (> 1000 - 2000 Å) makes them attractive model systems for studying chemical etching of thin metal films. In the present work, MTJ stacks typically possessed the layers shown in Fig. 1, and were deposited using either physical vapor deposition (PVD) or related methods.. The fixed-moment magnetic layer of $Co_{90}Fe_{10}$ is followed by a thin Al layer (e.g., 8-16 Å) which is then oxidized, e.g. by using an O_2 plasma, to form the AlO_x tunnel barrier.

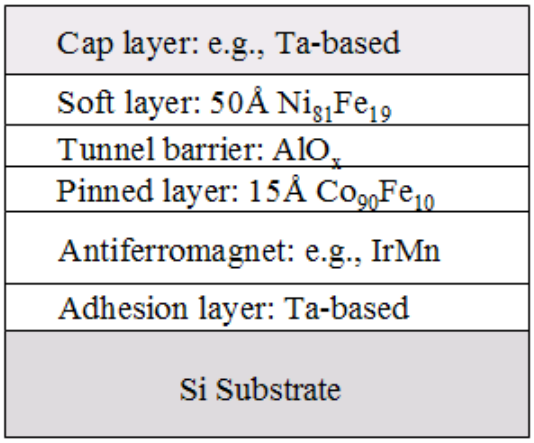

Figure 1. Schematic representation of a magnetic tunnel junction.

The options for patterning the MRAM stack typically include ion beam etching (IBE), reactive ion etching (RIE), chemical (wet) etching, or a combination of these

methods. Each etching method is not without problems. Thus, IBE, being a purely physical etching method, is non-selective, and material redeposition is a major problem. Halogen gas-based RIE methods cleanly chemically etch valve-metal-based layers, such as Ta, but will not chemically etch Permalloy at significant rates in low-density plasma environments.

Due to the thin nature of the FM films, lateral etching should be minimal, although Galvanically-enhanced etching of the pinned layer should be expected if care is not taken. The MTJ FM films ideally require weak etchant solutions in order to facilitate controlled etching, minimal lateral etching, and etch selectivity. However, with such solutions, surface passive films play a major role in the etching behavior of air- and reactive ion etch (RIE)-exposed FM films, in particular Ni-alloy layers. This paper describes initial fundamental chemical etching results for Permalloy ($Ni_{81}Fe_{19}$) in MTJ stack and single layer configurations, and the interplay between passivation, resulting from the preceding cap layer patterning step, and film dissolution.

Ti-Capped Permalloy Soft Layers

Early MRAM stacks at IBM utilized Ti as a capping layer on the Permalloy soft layer (see Fig. 1). Generally Ti films may be etched or patterned using either fluorine-based RIE or HF-containing solutions. However, etching thin Ti layers (in this case 100 Å thick) in a controlled manner using dilute (e.g. $\leqslant$ 0.1 mol dm^{-3}) HF solution was difficult owing to the passive oxide film on the Ti surface which appeared to grow over the course of 24 hr following PVD-type deposition. Thus, chemical etching of thin Ti layers in dilute HF solution was characterized by a variable induction period relating to dissolution of the passive film, followed by rapid dissolution of the unoxidized Ti.

To overcome the inhibiting effect of the Ti passive film, the Ti-capped stacks were first subjected to a CF_4/Ar(10 %) plasma to remove the surface film. Within ca. 2 hours, the remaining Ti was etched in the aqueous solution shown in Table I. In this solution, the succinic acid and sodium fluoride combined to provide a buffered source of HF to etch Ti. Benzotriazole (BTA) chemisorbed on newly-exposed $Ni_{81}Fe_{19}$ inhibiting its dissolution, thus enabling it to be etched in a solution selective to $Ni_{81}Fe_{19}$. Benzotriazole, which has long been used as a corrosion inhibitor for Cu (where it forms a $(Cu[I]\text{-}BTA)_n$ layer) evidently chemisorbed on the Permalloy surfaces. Complete removal of Ti in the RIE plasma resulted in a passivated $Ni_{81}Fe_{19}$ surface which inhibited etching in solutions other than those of strong acids or those containing oxidants that promote dissolution rather than passivation.

An objective of the present work was to develop a soft layer etching process that did not etch past the alumina tunnel barrier and etch the $Co_{90}Fe_{10}$ pinned magnetic layer (which is considerably more reactive than Permalloy). This ruled out conventional acid etchants such as sulfuric acid which caused the alumina barrier (bulk alumina is mildly basic with a pH of zero charge (PZC) of ca. 9.0) to etch rapidly, e.g. in $\leqslant$ 1

Table I. Ti Etching Solution	
Succinic acid	0.1 mol dm^{-3}
NaF	0.05 mol dm^{-3}
Benzotriazole	0.1 mol dm^{-3}
Thiourea	10 ppm
pH	4.3
Temperature	25 EC

min in 0.02 mol dm^{-3} H_2SO_4. Thus, attention was turned to aqueous solutions of carboxylic acids, in particular α, ω-dicarboxylic acids, some of which are listed in Table II. Immersion of the RIE-exposed $Ni_{81}Fe_{19}$ in a dilute solution of dicarboxylic acid, e.g. of concentration 0.01 – 0.1 mol dm^{-3} at pH 4 – 5, resulted in ready dissolution of the $Ni_{81}Fe_{19}$ layer (2 Å/s rate). Thiourea-related species chemisorbed on the $Ni_{81}Fe_{19}$ surface were critical for initiation of Ni81Fe19 dissolution in the weak dicarboxylic acid etchant. Throughout this work, the pH of these solutions was maintained in the 4 – 5 range in order to, as much as possible, reduce alumina tunnel barrier dissolution.

Completion of $Ni_{81}Fe_{19}$ layer etching was confirmed using sheet resistance and vibrating sample magnetometry (VSM) measurements, and X-ray photoelectron spectroscopy (XPS). Following Ti etching, the presence of a distinct, chemisorbed TU-related S species was confirmed by XPS (Fig. 3(a)). This species prevented the formation of a passivating layer on the $Ni_{81}Fe_{19}$ surface during DI water rinsing. In contrast, Permalloy did not etch if TU was omitted from the Ti etch solution (see Fig. 3(b)).

Table II. Etching Solutions: α, ω-dicarboxylic acids, $HOOC(CH2)_nCOOH$

Acid	n
Malonic	1
Succinic	2
Glutaric	3
Adipic	4
Glutaric	5
Suberic	6
Azelaic	7

Stopping the etching at the tunnel barrier avoids Galvanic corrosion reactions (due to the reactive fixed moment layer being in contact with noble metal-based AF one). If the alumina tunnel barrier thickness exceeded ≥ 12-15 Å[1], and was well formed (well oxidized, pinhole-free), etch selectivity was such that the more reactive fixed-moment $Co_{90}Fe_{10}$ located beneath the barrier remained intact. This was confirmed by VSM, and XPS. Figure 4 shows XPS data recorded at two different angles following soft layer removal in a suberic acid solution; it shows that the alumina tunnel barrier and the $Co_{90}Fe_{10}$ pinned layer are present . The dicarboxylic acids, $HOOC(CH_2)_nCOOH$, with n = 5 – 7 (Table II), which do not form stable chelate ring complexes with Al^{+3}, reacted least with alumina, as compared to, e.g., malonic acid (n = 1), which can form relatively stable 6-membered chelate ring compounds with Al^{+3}. The solubility of these acids in aqueous solution is strongly dependent on the value of "n"; the solubility of azelaic acid is essentially too low for practical use. Suberic acid was the etchant favored in this work.

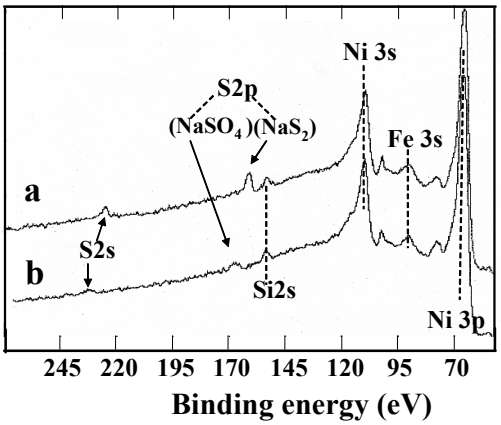

Figure 3. XPS characterization results for a) Permalloy surface after Ti etchant solution + TU, and b) TU-free etchant.

Ta-Capped Permalloy Soft layers

Compared to Ti, Ta cap layers impart improved properties to MRAM stacks, but may only be patterned using

[1] The final thickness of the AlO_x tunnel barrier is implied here, not the original Al thickness.

a RIE plasma containing reactive halogen species rather than by conventional chemical etching. Magnetic tunnel junction stacks with CF_4/Ar–patterned Ta cap layers did not exhibit $Ni_{81}Fe_{19}$ dissolution in suberic acid etchant. However, the use of SF_6 gas in place of CF_4 during RIE patterning of the Ta resulted in the $Ni_{81}Fe_{19}$ soft layers readily dissolving in the latter solution. X-ray photoelectron spectroscopy confirmed the presence of minute amounts of S on the surface of $Ni_{81}Fe_{19}$ following Ta removal. The chemisorbed S species caused the passive film formed on Permalloy at the conclusion of RIE etching of the Ta and during subsequent exposure to air to poorly protect the Permalloy. If improper activation of the $Ni_{81}Fe_{19}$ surface occurred during RIE, then incomplete etching subsequently occurred in solution; the $Ni_{81}Fe_{19}$ underwent passivation rather than etching reactions.

Physical Characteristics of Etched Junctions

A practical MRAM chip also has to have a sufficiently tight distribution of switching fields in order to allow selection of a particular bit in the writing process. A useful figure of merit for write yield is the "array quality factor" (AQF), which is defined as the ratio of mean switching field to the standard deviation of the switching field for the tunnel junctions in the MRAM device. Calculations show that write failures will occur if AQF is less than approximately 20. These failures are either half-select errors (flipping occurs when only the word or the bit line field is applied) or full-select errors (flipping does not occur even when both word and bit line fields are applied to the bit). Thus, high AQF is a critical requirement for successful MRAM operation, and is in practice strongly influenced by the quality of the MTJ definition process.

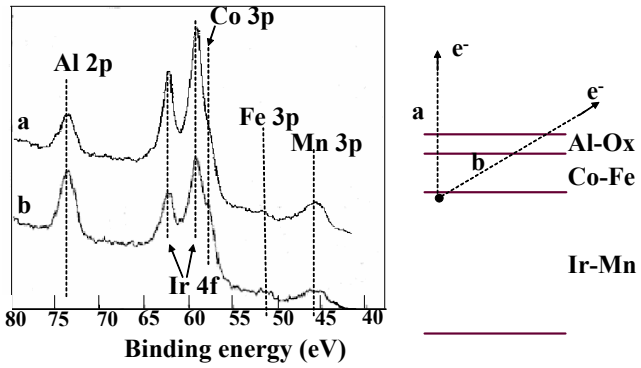

Figure 4. XPS spectra for MTJ stack following soft layer etching. Spectrum a) was recorded at a 90° angle, while b) was recorded at an angle < 90°.

The magnetic behavior of MRAM elements is strongly dependent on shape anisotropy. Figure 5 shows top-down SEM micrographs of ion milled and wet etched Ta-capped MRAM elements. The latter were formed from sputter deposited films of the following type: Si | SiO_2 | Ta (100 Å) | $Ni_{81}Fe_{19}$ (50 Å) | Ta (100 Å). The ion milled junction (Fig. 5(b)) exhibits blunt points, and contains redeposited material, or "fences", represented by the white region at the element perimeter.

The wet etched MRAM element (Fig. 5(a)) exhibits better shape characteristics than the ion milled element. This is a consequence of using a chemically efficient RIE process to first pattern the Ta cap layer, and hence, no fence material is evident at the edges of the element.

A TEM image of a cross-section of part of an etched element is shown in Fig 6. In this case, a ternary alloy, $Ni_{65}Fe_{15}Co_{20,}$ rather than Permalloy, was used as the magnetic layer. The top Ta layer was again patterned using RIE. The TEM image shows that little

lateral etching occurred for the ternary alloy layer, which is visible in the image between the darker, higher-mass Ta layers. A passive oxide film is visible on the Ta mask, and also on the bottom Ta layer exposed on etching away the magnetic layer.

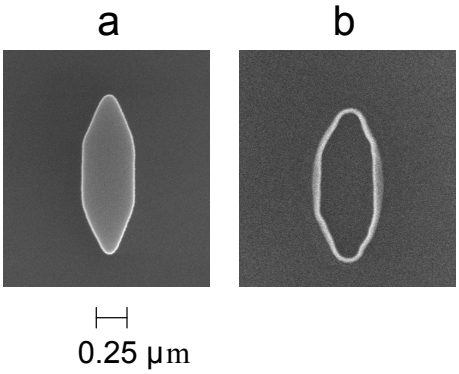

Figure 5. SEM images of a chemically-etched MRAM element (a) and an ion milled element (b).

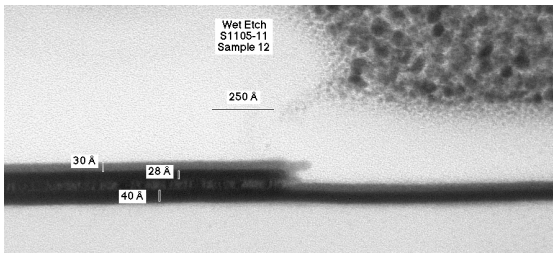

Figure 6. TEM cross-section of a chemically-etched MRAM element of the following type: Si | SiO_2 | Ta (40 Å) | $Ni_{65}Fe_{15}Co_{20}$ (50 Å) | Ta (40 Å).

Magnetic Behavior

A hysteresis loop, recorded using alternating gradient magnetrometry (AGM), is shown in Fig. 7 for an array of Permalloy elements. The data represent the average hysteresis behavior recorded for about 2 million elements (each 0.28 µm x 1.4 µm). This curve shows a mean coercivity (H_c) of 103 Oe, and a sharp, average transition characterized by a switching field standard deviation value σ of 3.7 Oe.

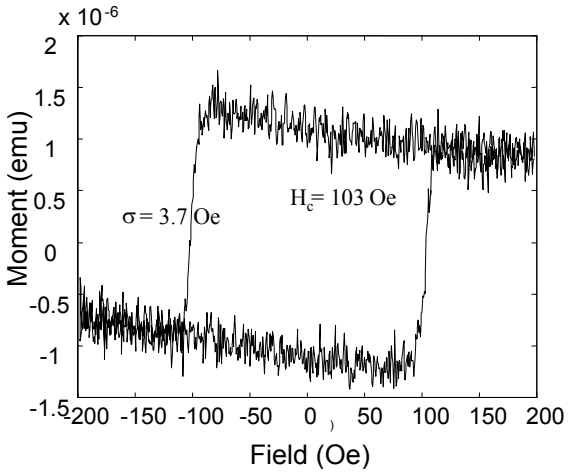

Figure 7. AGM hysteresis loop for a chemically etched array of magnetic elements made from the following thin film stack: Si | SiO_2 | Ta (50 Å) | $Ni_{81}Fe_{19}$ (50 Å) | Ta (50 Å). Etchant: 0.05 mol dm^{-3} suberic acid at pH = 5; time = 8.0 min.

The ratio H_c/σ, or "array quality factor" (AQF), is an indicator of the quality of magnetic switching. The AQF value derived from the curve in Fig. 7 is ca. 28. As indicated earlier, an AQF value in excess of about 20 is needed in practical MRAM devices to avoid write failures. The results in Fig. 7 indicate that chemical etching has promise for patterning MRAM magnetic layers.

Figure 8 shows switching field distribution data for a range of etch times for an array of Permalloy elements which were of size 0.28 µm x 1.4 µm. The AQF data displayed

in Fig. 8(c) was obtained from the switching field data and spread data in Figs. 8(a) and 8(b), respectively. The AQF values increased with etch time, indicating that the magnetic switching properties of the array of elements improved with etch time, i.e., the range of switching fields exhibited by the array of elements tightened. To attempt to explain this result, it is worth discussing the data in Figs. 8(a) and (b).

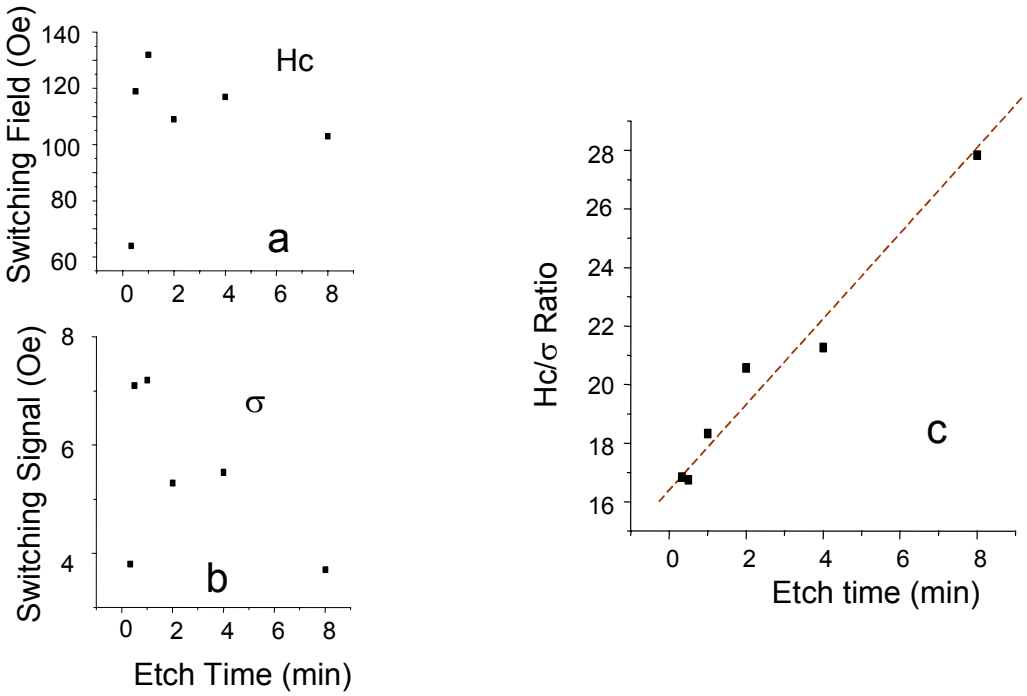

Figure 8. Array switching distribution behavior versus etch time. Data obtained using AGM method. Magnetic stack was of the following composition: Si substrate | SiO_2 | Ta (50 Å) | $Ni_{81}Fe_{19}$ (50 Å) | Ta (50 Å).

The switching field, or Hc, data in Fig. 8(a) shows a maximum at about one minute of etching time and then remains unchanged for longer etch times, or shows a gradual decrease. This is a surprising result, since one would expect Permalloy etching to continue and, as the diameter of the Permalloy elements decreased, Hc to increase. Either some unascertained change in the properties of the Permalloy elements occurred, such as in element aspect ratio, shape or magnetization, or a drastic decrease in, or ceasing of, Permalloy etching occurred at the element edges. Of significant interest is the fact that the switching field distribution actually tightened (Fig. 8(b)) with increase in etch time. This trend is somewhat surprising considering that for all of the etch times reported the inter-element regions of the films were completely etched, as indicated by the relatively constant switching field shown in Fig. 8(a). The further improvement in σ is likely due to improved TJ edge smoothness (due to preferential etching at remaining actives sites, including the two pointed regions of the Permalloy elements). Finally, the increase in AQF with etch time at longer times was mainly driven by the decrease in the value of σ, and surprisingly was not helped by increasing values of Hc. For MRAM applications, increasing values of Hc with etch time would not be desirable, since higher write currents would have to be employed in MRAM devices to generate the appropriate switching fields.

Etching thin films of Permalloy (e.g. ⩽ 100 Å thick) containing trace amounts of S additive chemisorbed on the surface (in this instance derived from the SF_6 RIE gas) is likely to proceed at a more rapid rate than etching bulk, or thick film, Permalloy. When etching thick-film Permalloy in a weak etchant, such as suberic acid solution at pH 4 – 5, competition may develop between dissolution into solution and growth of a passive film. The latter may drastically slow Permalloy element etching, since dissolution of the passive film is then relied upon to promote Permalloy etching. In the case of Permalloy, O_2 gas oxidant dissolved in solution may promote growth of a metastable passive film, which undergoes dissolution at a slow rate. In the limiting case of a passive oxide film inhibiting dissolution, Permalloy films which did not contain a Ta cap layer but which were exposed to air (oxygen plus humidity), did not undergo dissolution in the acid etchants employed in this work.

Figure 8(b) shows that the switching signal (σ) also exhibits a maximum at about one minute, and then decreases at longer etch times. A possible explanation for the trend in the data for σ is that Permalloy etching was incomplete at the shorter etch times, and that either a ragged profile, or device-to-device variations, contributed to greater switching non-uniformity. However, as etch time increased, the etching rate, i.e. at element edges, of initially-formed elements apparently slowed, and those elements which originally lagged in definition continued to be etched. Further smoothing of the edges would also be expected, thereby reducing switching field spread. It is possible that there was initial non-uniformity in the process of patterning the Permalloy elements since, a) a weak etchant was employed which would have initially etched more active regions of the Permalloy surface, and b) local, or pattern-dependent, non-uniformity may have been a feature of the preceding RIE step. In the case of the latter step, it is possible that trace amounts of Ta may have remained on regions of the Permalloy surface, and a non-uniform distribution of activating S additive on the Permalloy surface may also have resulted.

All MRAM films were deposited using PVD methods on Si wafers. The alumina tunnel barriers were formed by exposing Al layers to air. Reactive ion etching was carried out in a PlasmaLab μP tool. Mask creation was carried out using either standard photoresist processing methods, or ebeam lithography methods. Reagent grade chemicals and 18 Mega Ohm DI water were employed. Magnetic film etching was confirmed using sheet resistance and vibrating sample magnetometry (VSM) measurements, and X-ray photoelectron spectroscopy (XPS).

NON-MRAM METAL FILMS

Wet chemical etching can be an enabler for, and be enabled by, newly emerging technologies. An example is found in the field of “microcontact printing” (μCP; a “soft lithography” technique) which uses self-assembled monolayers (SAMs) as masks. The formation of passivating films enables the technologically important process of metallic film removal via chemical mechanical planarization (CMP).

Self-Assembled Monolayer Masks

Chemical etching can serve as an important fabrication method in certain technologies, such as large-area substrate fabrication which requires inexpensive, high-

through-put processes, e.g., paper-like displays. Self-assembled monolayers (SAMs) deposited by micro-contact printing using elastomeric stamps are being explored as alternative, and higher resolution, pattern-transfer masks to the traditional polymeric resists. In the case of ebeam resists, imperfect, non-vertical patterning (beam broadening effects) tends to be observed for the relatively thick resist layers (e.g., approaching 1.0 μm in thickness). When spun as ultrathin films (e.g., a few nanometers thick), polymeric resists tend to have pinholes and other imperfections that allow etch solutions to create defects in the underlying film.

In the stamp contact regions, the alkanethiol preferentially reacts with the surface, typically Au, to form a dense monolayer. The layers form via spontaneous, thermodynamically-driven organization of molecules, which leads to films with low defect densities. This spontaneous tendency for self-organization is the crucial property that makes SAMS so interesting from a pattern transfer point of view: they naturally oppose formation of film defects and pinholes, substrate problems notwithstanding. Since plasma etches are likely to rapidly destroy such thin masks, chemical etching seems to be a natural match for SAM masks.

The stamps for μCP are typically made from elastomeric materials, such as polydimethylsiloxane (PDMS). The precursors of the stamp material are polymerized on a master (Fig. 9) defined by optical or ebeam lithography. After curing, the stamp is

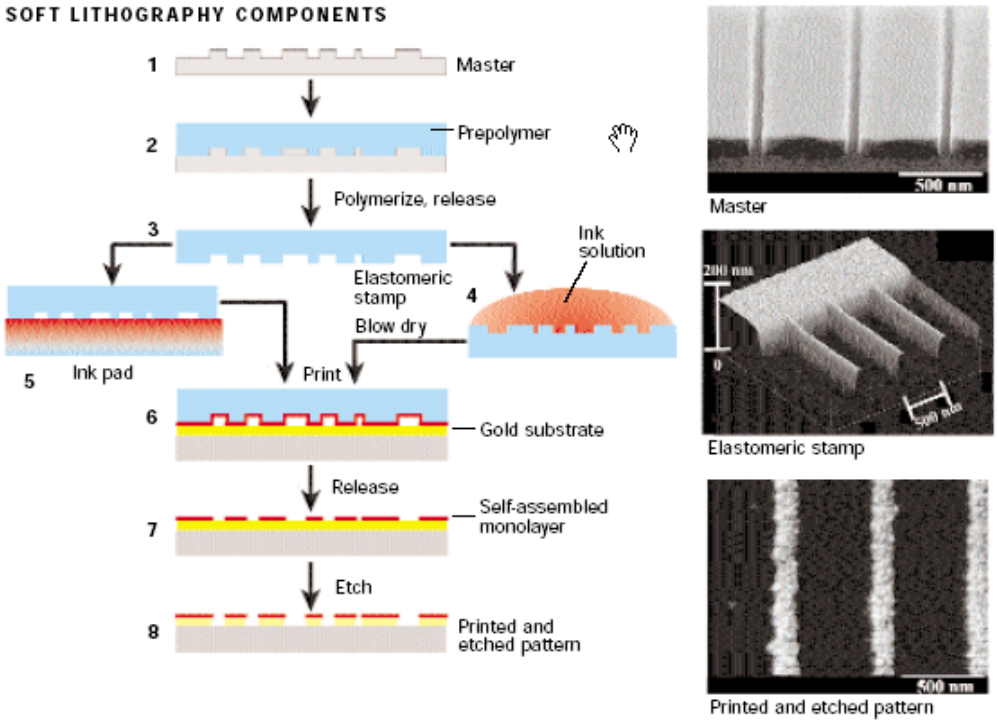

Figure 9. Process flow for microcontact printing alkanethiols on a gold substrate: a prepolymer (2) covering the master (1) is cured by light and demolded to form an elastomeric stamp (3), which is inked by immersion (4) or with an ink pad (5) and printed onto the substrate (6), forming a self-assembled monolayer, which is transferred into the substrate by a selective chemical etch. SEMs show the master, image of the stamp, and the printed and etched Au pattern. Adapted from ref. (6).

released from the mould, and the stamp pattern is impregnated with ink using an ink pad (left), or by applying ink solution (right). During printing, conformal contact between the relief pattern and the substrate allows localized transfer of the alkanethiol and the formation of SAMs. The chemical pattern of SAMs may then be transferred into the gold by a wet etch process.

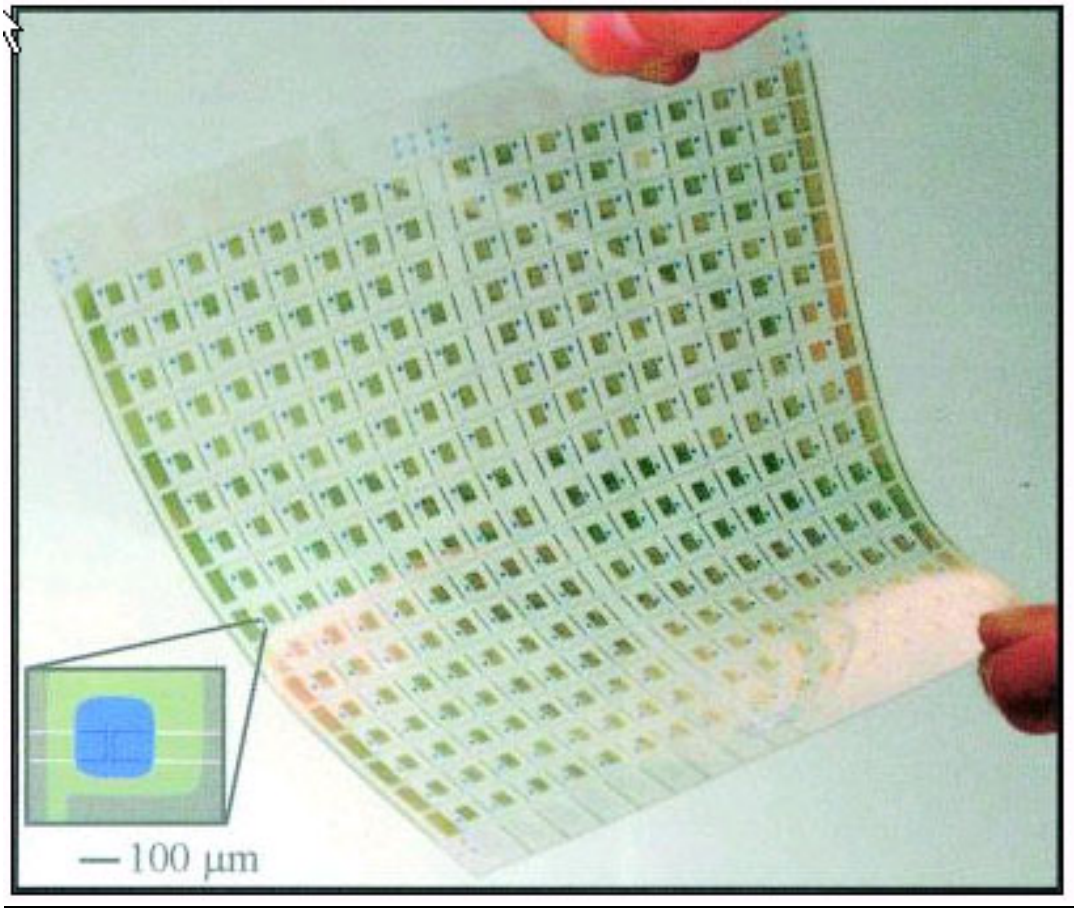

Figure 10. Image of a completed plastic active matrix backplane circuit. The *Inset* shows an optical micrograph of a typical transistor. Fabrication involved: a) using a rubber stamp to print an ink pattern of hexa-decanethiol (HDT); chemical etching of the gold, and Ti adhesion layer, to produce a conducting circuit pattern; and c) removing the SAM by baking at 150 ºC to enable electrical contact between these patterns and layers of organic semi-conductor deposited on top of them. Adapted from ref. (7).

A limitation of alkanethiols is that they self-assemble on a limited number of noble metal surfaces, principally Au and Ag, and Cu to form dense, ordered monolayers. The patterning of other materials, such as semiconductors, requires the use of a sacrificial Au mask. Such substrate restrictions notwithstanding, Rogers et al. (7) showed that it is possible to print high-quality, large-area plastic electronic systems on low-cost mechanically flexible polymer substrates (Fig. 10). They showed how rubber-stamped circuit elements can be combined with organic semiconductors to form active matrix backplanes for large sheets of electronic paper. They reported that the performance of these systems was excellent, i.e. the transistors had characteristics (e.g., on and off currents) that were comparable to, or better than, those of similar devices fabricated on

rigid silicon supports by using conventional photolithographic methods, and that the optical characteristics (e.g., switching time and contrast ratio) of the resulting displays were as good as those of low-resolution signs that use similar electronic inks and direct-drive dressing schemes.

An etch system can be made highly selective if at least one of the molecules necessary to etch the substrate cannot penetrate through defects, or pinholes, in the monolayer SAM resist. Defects are much more likely to be present in SAM layers formed on Cu than on Au. Michel and coworkers (8) found that an etching solution containing a branched polyethylenimine (PEI), which has primary and secondary amino groups, did not etch Cu through defects in the SAM layer. This selectivity was observed both in the case of relatively thin (100 nm) and thick (2.2 μm thick) Cu layers. Such selectivity could not be achieved using either the well known cyanide/O_2 etching solution, or one similar that used for Fig. 9, but with low molecular weight amine-type complexants.

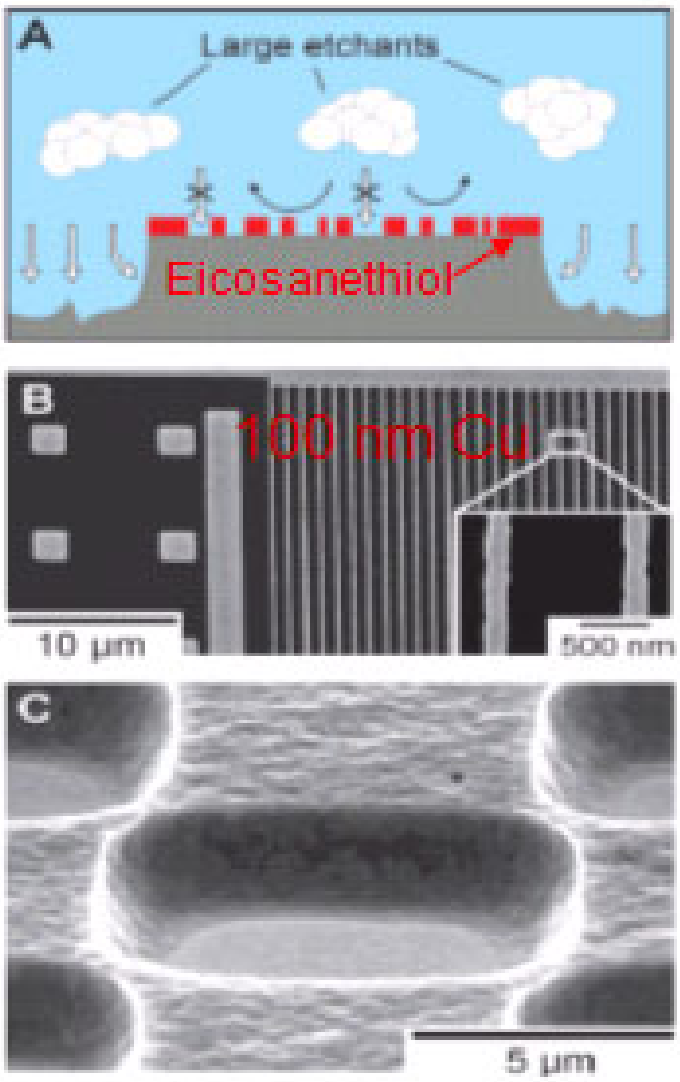

Figure 11.

A): Effect of large etchant molecules on maintaining etch selectivity in the presence of mask defects;

B): SEM image of micrometer-sized structures and 170-nm-wide nano-wires formed by etching a 100-nm-thick Cu substrate using a bath containing large PEI molecules;

C): The etch system remained selective even for etching a rough, 2.2 μm-thick, electrodeposited Cu film. Adapted from ref. (8).

The major disadvantage of wet etching through the ages has been its isotropic nature, which means it tends to be an impractical process for patterning films when feature sizes approach film thickness dimensions. While the development of practical, anisotropic, solution-based chemical etches is extremely challenging, Michel and coworkers (8) developed a wet etch process with directional properties for thick Cu layers that led to tapered feature sidewalls (Fig. 12). This process is based on competition between isotropic etching and diffusion of blocking additives, which form an etch barrier that spreads out from the mask edges over unprotected regions of the substrate. The etch barrier self assembles from additives in the bath, first over the patterned regions of the substrate, and then expands laterally outwards.

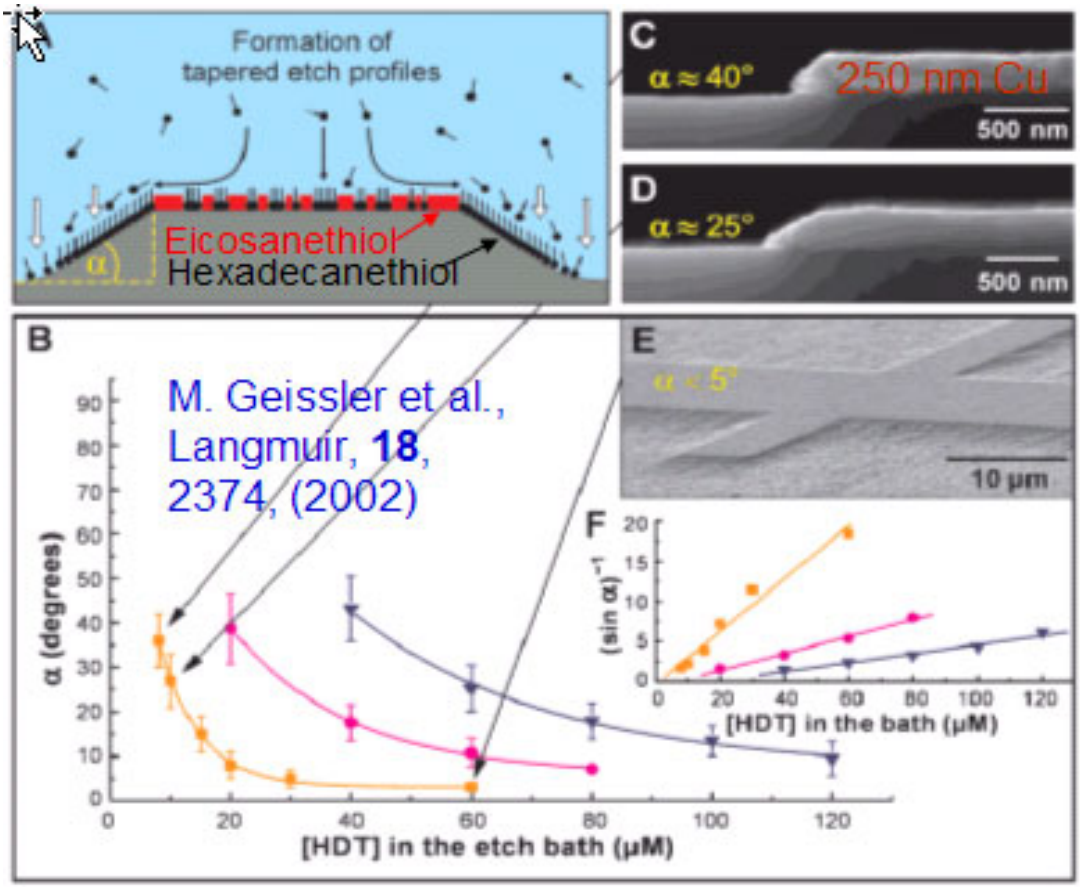

Figure 12. Competition between etching and diffusion of blocking additives can be used to taper structures. The data were obtained using a 250-nm-thick Cu film deposited on a Si wafer, which was printed with 0.2 mM solutions of eicosanethiol (ECT); the films were etched in a CN^-/O_2 solution containing C12E6 (0.2 mM), hexadecanethiol (HDT) additives, and an oxidant of varying concentrations: 0 (□), 0.2 mM (○), and 0.5 mM (▽). Adapted from ref. (8).

As shown schematically in Fig. 12(a), a SAM monolayer patterned on a substrate can direct the lateral growth of a mask formed from additives, resulting in a taper angle α. The taper depends on the strength of the etch bath and on the concentration of the additives. The lines in the graph are guides for the eye. The SEM cross-section images reveal taper angles of ~ 40º (C) and ~ 25º (D) for Cu patterns formed at the conditions

referenced in the diagram. Using a slow bath and a high concentration of HDT, it is possible to form low tapers, such as the one obtained in the 500-nm-thick Cu layer shown here(F). The ratio between the spreading of the resist and the rate of etching is equivalent to $(\sin a)^{-1}$, which represents the length of the taper sidewall divided by its height.

Chemical Mechanical Planarization

We have seen how passive films strongly impact, and complicate, wet chemical etching of thin Permalloy films. Passive films, however, play a critical role in the success of chemical mechanical planarization (CMP) of metal films

Due to its isotropic nature, wet etching is incapable of preferentially removing topographical features. Planarization is achieved by addition of a metal passivating agent and an abrasive agent. The purpose of the abrasive agent is to continually abrade the passivation layer in the high regions of the surface, while the low spots are largely protected. The passivation layer rapidly regrows through preferential metal dissolution into the layer rather than into solution. The competition between dissolution into the passive film and into solution is dependent on the CMP solution conditions. For some metal films, e.g. tungsten, a passive oxide can serve as the passivation layer. The passivation layer may also provide post-CMP corrosion protection. The original cyclical passivation-abrasion model for CMP was proposed for W by Kaufman and coworkers in 1991 (9).

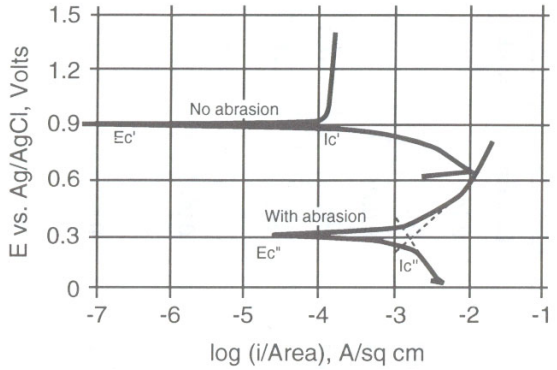

Figure 13(a). Polarization curves for W in the presence (lower curves) and absence (upper curves) of abrasion in 5 wt% $Ce(NO_3)_3/HNO_3$ CMP slurry. Adapted from ref. (10).

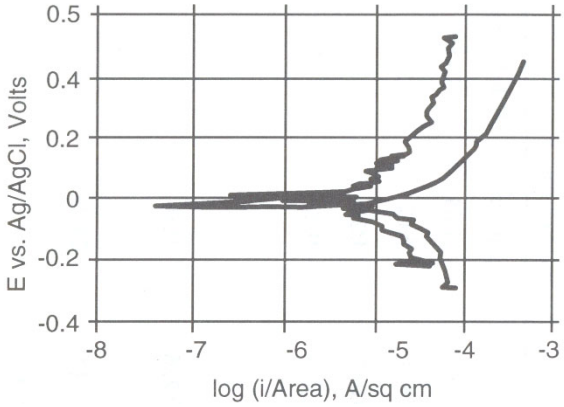

Figure 13(b). Polarization curves for W in 10 wt% H_2O_2-containing CMP slurry with and without abrasion. Adapted from ref. (10).

Tungsten CMP proceeds through an intermediate passive oxide which abrades readily during CMP (9). The likely film-forming reaction in the case of ferricyanide oxidant is as follows:

$$W + 6Fe(CN)_6^{-3} + 3H_2O = WO_3 + 6Fe(CN)_6^{-4} + 6H^+$$

The WO_3 is probably present in various extents of hydration depending on the slurry solution conditions, such as pH. Nevertheless, it is sufficiently protective to drastically reduce W dissolution and removal, unless abrasion is employed (Fig 13(a)). As shown in Fig 13(a), in the presence of abrasion, the W potential is about 600 mV more cathodic (i.e., in the direction greater activity), and the etching/corrosion current density appears to be about two orders of magnitude higher.

A protective passivation film does not form on W in H_2O_2 solutions, as confirmed by the closeness of the potential-current curves in Fig. 13(b) for the presence and absence of abrasion. This lack of protective behavior is a consequence of the ready reaction of the tungsten oxide film species with peroxide to form soluble complexes. This reactivity is similar to the well-known etching reaction of peroxide with Ti (11).

Being more noble, Cu shows less tendency than W to become passivated. However, the passive oxide film formed in certain H_2O_2-containing slurries significantly slows chemical etching, while in other, non-H_2O_2-type slurries, Cu dissolution has to be controlled by film-forming additives. At low H_2O_2 concentrations (< 1%), Cu removal tends to be dominated by chemical etching; at high H_2O_2 concentrations, Cu removal is controlled by mechanical removal of the oxide passive film. As shown in Fig. 14(b), the open circuit potential of Cu is significantly more cathodic in the presence of abrasion for the case of 1.0% H_2O_2. As shown in Figs. 14(c) – (d), at higher concentrations of H_2O_2, the passive film reforms virtually instantly during abrasion, resulting in less difference in open circuit potential between the abrasion-free and abrasion cases.

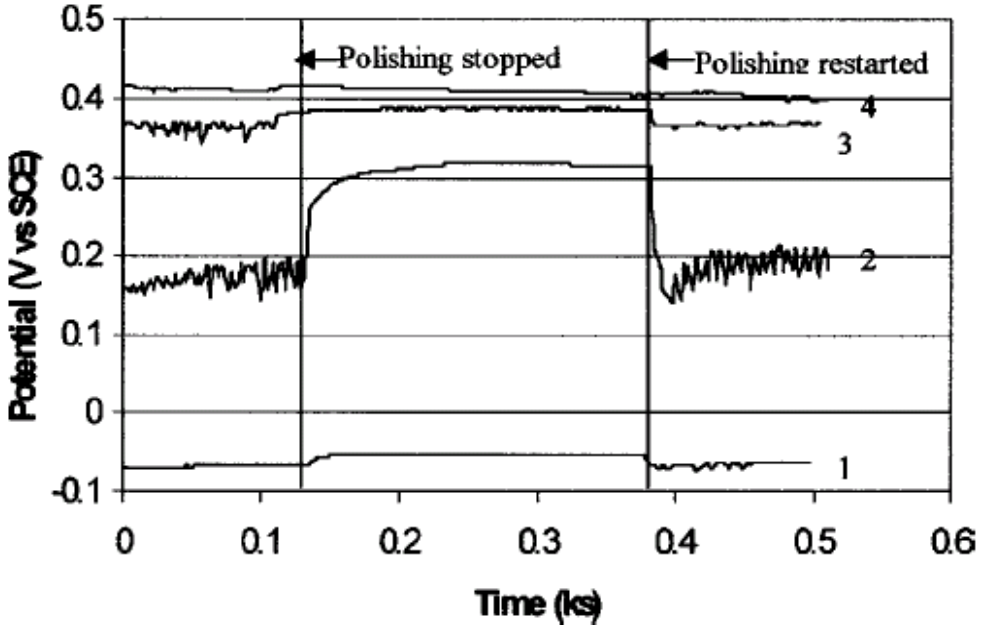

Figure 14. Open circuit potential curves recorded for Cu in CMP slurries containing various concentrations of H_2O_2. 1: no H_2O_2; 2: 1% H_2O_2; 3: 5% H_2O_2; 4: 10% H_2O_2.

An interesting feature of H_2O_2 slurries is that Cu has been found to passivate at slurry solution pHs where formation of an oxidized solid phase is not expected from the potential-pH, or Pourbaix diagram (12). This has been ascribed to either pH increase at the surface due to H_2O_2 reduction, or to formation of the powerful oxidant radical $HO^{\bullet}$ due to H_2O_2 decomposition (13). The formation of the $HO^{\bullet}$ radical is thought to be catalyzed by Cu(II) ions, especially when complexed by amino acid ligands.

Several oxidizers, e.g. $FeCl_3$ and $NH_4S_2O_8$, freely etch Cu. Dissolution has to be controlled by additives, e.g. BTA, capable of forming protective films, e.g., Cu(I)-BTA. The latter imparts much-needed, enhanced, post-CMP corrosion resistance to the surface of the Cu features.

A key feature of Cu CMP development is the drive to reduce the extent of the mechanical abrasion component of CMP in order to integrate soft, low-dielectric-constant dielectrics in the Cu- BEOL process.

CONCLUSIONS

Chemical etching shows promise for selective patterning of magnetic soft (or free) layers, principally Permalloy, in MRAM stacks. Passive films formed in the prior cap layer patterning step play a critical role in the etching behavior of the magnetic layers. The novel use of a sulfur-based additive to inhibit Permalloy passivation, thus enabling selective etching in weak acid etchants, was demonstrated. Aqueous etch solutions of α, ω-dicarboxylic acids were found to etch Permalloy films whose surfaces contained a chemisorbed, sulfur-based, passivation inhibitor. The longer chain dicarboxylic acids, especially suberic, not alone etched Permalloy but left intact the alumina tunnel barrier and the underlying "pinned" magnetic layer. High values of array quality factors for magnetic switching were demonstrated for chemically etched arrays of Permalloy elements.

Wet chemical etching can be an enabler for, and be enabled by, newly emerging technologies. This is clearly evident in the field of "microcontact printing" (μCP; a "soft lithography" technique) which uses self-assembled monolayers (SAMs) as masks. The ability to taper feature sidewalls in the case of Cu layers, and thus somewhat overcome the isotropic nature of chemical etching, is an important advancement.

As the drive toward less-aggressive, lower-downforce CMP continues in order to integrate soft low-dielectric-constant dielectrics, passive films, both oxide and inhibitor based, will continue to be critically important in controlling dissolution in the low-lying regions of substrate wafers during the CMP process.

ACKNOWLEDGEMENTS

The authors gratefully acknowledge S. Parkin, A. Gupta, and S. Brown for films; D. Abraham for measurements of magnetic properties; A. Schrott for XPS characterization;

P. Rice (IBM Almaden) for TEM analysis; experimental help from B. Varghese and P. Bhatnagar; W. Gallagher and A Gupta for discussions and encouragement; DARPA for partial support of this work.

REFERENCES

1. S.S.P. Parkin et al., *Proc. IEEE*, **91**, 661 (2003).
2. E.J. O'Sullivan, paper in this proceedings volume.
3. B.N. Engel et al., *IEEE Trans. Nano.*, **1**, 32 (2002).
4. R.P. Cowburn, *Materials Today*, **July/August**, 32 (2003).
5. E.J. O'Sullivan and A. Schrott, *U.S. Patent* 6,426,012 (2002).
6. B. Michel, et al., *IBM J. Res. Dev.,* **45**, 697-719 (2001).
7. J. Rogers, et al., *Proc. Natl. Acad. Sci. USA*, **98,** 4835-4840 (2001).
8. M. Geissler et al., *Langmuir,* **18(6),** 2374-2377 (2002).
9. F. Kaufman, et al., J. *Electrochem. Soc.,* **138**, 3460 (1991).
10. J. Farkas, et al. in "*Adv. Metal. For ULSI Applications*", ed. by R. Blumenthal and G. Jannsen (Mat. Res. Soc., Pennsylvania, 1995).
11. S. Verhaverbeke et al., *Mat. Res. Soc. Symp. Proc*., **477**, 447 (1997).
12. M. Pourbaix, *"Atlas of Electrochemical Equilibria in Aqueous Solutions",* Pergamon Press, London, 1965, p. 384.
13. M. Hariharaputhiran et al., *J. Electrochem. Soc.,* **147**, 3820 (2000).